

1995

## A New Model of Low Temperature Photoluminescence in Amorphous Semiconductors

Mathieu Kemp

*Northwestern University, Evanston, Illinois*, lechat@chem.nwu.edu

Marvin Silver

*University of North Carolina, Chapel Hill*

Follow this and additional works at: <https://digitalcommons.usu.edu/microscopy>

 Part of the [Biology Commons](#)

### Recommended Citation

Kemp, Mathieu and Silver, Marvin (1995) "A New Model of Low Temperature Photoluminescence in Amorphous Semiconductors," *Scanning Microscopy*: Vol. 1995 : No. 9 , Article 5.

Available at: <https://digitalcommons.usu.edu/microscopy/vol1995/iss9/5>

This Article is brought to you for free and open access by the Western Dairy Center at DigitalCommons@USU. It has been accepted for inclusion in Scanning Microscopy by an authorized administrator of DigitalCommons@USU. For more information, please contact [digitalcommons@usu.edu](mailto:digitalcommons@usu.edu).



## A NEW MODEL OF LOW TEMPERATURE PHOTOLUMINESCENCE IN AMORPHOUS SEMICONDUCTORS

Mathieu Kemp\* and Marvin Silver<sup>1</sup>

Department of Chemistry, Northwestern University, Evanston, IL 60208-3113

<sup>1</sup>Department of Physics and Astronomy, University of North Carolina, Chapel Hill, NC 27599-3255

### Abstract

Recent low temperature a-Si:H photoluminescence experiments show the presence of two peaks in the lifetime distribution, and a dependence of the efficiency on generation rate. These results contradict every existing model of amorphous semiconductor photoluminescence. The reason for the discrepancy is that every model predicts diffusive motion of the photo-generated pairs. We show how the inclusion of coulomb interaction between photocarriers, spin selection effects, and Auger recombination gives back agreement of theory with experiment. This new picture of the phenomenon also explains the transient behavior of the luminescence intensity.

**Key Words:** Luminescence, photoluminescence, luminescence modeling, low temperature luminescence, spin dependent luminescence, recombination, geminate recombination, semiconductors, amorphous semiconductors, amorphous silicon.

### Introduction

Recent advances in the experimental investigation of low temperature photoluminescence (PL) in amorphous semiconductors have revealed a series of puzzling facts which contradict preexisting models of the phenomenon. The most important of these are:

(1) The existence of two lifetime peaks at  $3 \times 10^{-3}$  seconds (s) and  $3 \times 10^{-6}$  s. The peaks are 2 decades wide. The amplitude of the slow peak is three times larger than that of the fast peak (Ambros *et al.*, 1991).

(2) The existence of a low generation rate geminate regime (Bort *et al.*, 1991).

(3) The lifetime dependence on generation rate (G). At low G, the lifetime is constant; at high G, the lifetime decreases as  $G^{-1/2}$ . Both PL channels have the same G dependence, however the generation rate for the onset of the fast channel lifetime shortening is 1000 times larger than that of the slow channel (Ambros *et al.*, 1991).

(4) The dependence of the efficiency follows the dependence of the lifetime on G (Ambros *et al.*, 1991).

At present, four PL models have been suggested, none of them successful in explaining the data. The first three assume that the lifetime broadening is the result of pair separation broadening. Energy Loss Hopping (ELH) makes pair broadening the result of a random walk on the manifold of localized electronic states (Shklovskii *et al.*, 1989). This model contradicts the observations of two lifetime peaks and two narrow peaks. The Distant Pair (DP) model assumes that pairs are spatially randomized after photogeneration and that their density determines the lifetime (Dunstan, 1982). This model is in contradiction with the observations of (i) geminate recombination, (ii) the presence of two peaks, and (iii) independence of the lifetime on pair density at low generation rate. It also requires (iv) very large carrier densities, 10 times larger than that which is observed ( $10^{17} \text{ cm}^{-3}$  compared with  $10^{16} \text{ cm}^{-3}$ ; see Bort *et al.*, 1991). Coulomb Assisted Recombination (CAR) is similar to ELH, with the difference that the coulombic interaction between photogenerated electron and hole is

\*Contact for correspondence:

Mathieu Kemp, address as above.

Telephone number: (847) 491-3423

FAX number: (847) 491-7713

E.mail: lechat@chem.nwu.edu

explicitly taken into account (Kemp and Silver, 1992). Like ELH, it predicts one lifetime only, however, of the correct width. Finally, Transport Controlled Recombination (TCR) is similar to ELH and CAR; however, it relaxes the assumption that the lifetime is determined by the radiative tunneling transition (Kemp and Silver, 1992). TCR predicts (i) two lifetime peaks, the fast one corresponding to reaction limited recombination, and the second, to diffusion limited recombination, (ii) the correct position and width of the fast peak, and however, (iii) a very broad slow recombination channel.

The problem of the width, particularly the width of the slow recombination channel, occurs in most models. It is becoming apparent that this is a quasi-unavoidable feature of the hopping formulation. The source of the problem is the assumption that the pair broadening is due to the diffusion of the photocarriers between generation and recombination. To illustrate this, consider that a lifetime ( $\tau$  = typical radiation lifetime) width of 2 decades translates into a pair separation broadening of

$$\Delta r = \{[\lambda/2][\log(10)][\Delta \log_{10}(\tau)]\} \cong 12 \text{ angstroms.} \quad (1)$$

Here, we assume that the radiative tunneling transition controls the lifetime, and a typical localization length  $\lambda = 15 \text{ \AA}$ . We also use the fact that the experimental method accounts for about 1.5 decades of the total broadening. This number is compared with the average spacing between localized states, which sets the length scale for the diffusion process. For a density of localized states  $N_s = 5 \times 10^{19} \text{ cm}^{-3}$ , the average spacing is  $27 \text{ \AA}$ . This is twice the observed number! Therefore, if a dynamical formulation is to give agreement with experiment, it cannot be based on a diffusive type of random walk, as is the case in most amorphous semiconductor PL models. The corollary to this is a consistent account of the data must be based on a type of dynamics that focuses the pair separation.

CAR is the only model that predicts focusing behavior. This is due to the coulomb interaction between electron and hole, which forces the pair separation to decrease. CAR shows that the pair separation decreases until the electron occupies the closest localized site to the hole. When this is the case, the pair separation prior to recombination is the nearest-neighbor distribution, and the half-peak width is:

$$\Delta r = 0.5(N_s)^{-1/3} \cong 14 \text{ angstroms.} \quad (2)$$

Comparison with eq. (1) shows that this is much closer to the experimental value. This simple observation gives strong support to the central importance of the coulomb interaction in PL.

As we mentioned, the problem with CAR is its prediction of one peak and not two. If we assume that the lifetime is determined by the final jump, then the CAR lifetime peak ( $\tau_{\text{peak}}$ ) is located at:

$$\tau_{\text{peak}} = \tau_0 \exp(2r_{\text{peak}}/\lambda), \quad (3)$$

where the prefactor  $\tau_0$  is of order  $10^{-7}$  s. Since the peak of the nearest neighbor distribution function occurs at  $r_{\text{peak}} = 0.54N_s^{-1/3}$ , this gives:

$$\tau_{\text{peak}} \approx 7\tau_0. \quad (4)$$

This number does not compare well with experiment (the slow peak occurs at  $3 \times 10^{-3}$  s). On the other hand, it gives the right order of magnitude for the fast peak ( $3 \times 10^{-6}$  s).

Ambros *et al.* (1991) have suggested that each lifetime peak corresponds to a different recombination channel. They also suggested this to be the result of spin statistics or of potential fluctuations. The suggestion of spin statistics is attractive for three reasons. First, it predicts two independent transitions, an allowed and a forbidden. Second, the lifetime of the forbidden transition is much longer than that of the fast one. Finally, in the absence of magnetic bias and for lifetimes long compared with the spin flip time, the forbidden transition is 3 times more frequent than the allowed one (3 triplet states compared to 1 singlet). Like Ambros *et al.* (1991), we will assume PL is subject to spin selection rules. We will assume there are 2 radiative rate prefactors, the singlet,  $\tau_0^s$ , of order of  $10^{-7}$  s, and the triplet,  $\tau_0^t$ , of order  $1000 \tau_0^s$ . This generalization of CAR should give two peaks, located at the correct positions, with the correct widths, and in the correct ratio.

The second important aspect of the experimental data is that the PL efficiency decreases with increased generation rate, and the evolution with G of the efficiency mirrors that of the lifetime. The importance of this observation lies in the fact that it disagrees with all previous models of PL. In every PL model, the lifetime shortening has been assigned to non-geminate recombination, i.e., to the effect of reduced interpair separation. Common to all these models is the assumption that the efficiency is solely controlled by defects, and as a consequence, is unity at low defect density. This contradicts experiment. The data clearly shows the presence of a non-radiative mechanism, even for high quality samples. Furthermore, the data supports the conclusion that shortening of the lifetime is correlated with efficiency.

Street (1984) has suggested Auger recombination as a possible non-radiative recombination mechanism. The  $G^{-1/2}$  dependence of the efficiency observed by Ambros *et al.* (1991) is in direct support of this. The argument

in favor of Auger goes as this: if  $\tau$  is the typical radiative lifetime, then assuming Auger to be competing with radiative recombination,

$$(dn/dt) = \{G - (n/\tau) - An^2\}. \quad (5)$$

where  $A$  is a proportionality constant, and  $n$  the carrier density. In the steady-state and for dominant Auger, the efficiency is:

$$\eta = \{(n/\tau)/(An^2)\} \approx G^{-1/2}, \quad (6)$$

and the lifetime:

$$\tau_{\text{peak}} = (1/An) \approx G^{-1/2}. \quad (7)$$

When Auger can be neglected, the efficiency is unity, and the lifetime is  $\tau$ . The transition to Auger dominated PL occurs at

$$G_{\text{threshold}} = 1/A\tau^2. \quad (8)$$

A similar set of equations holds for the fast peak. In view of the agreement of this with experiment, we believe, along with Street (1984) and Ambros *et al.* (1991), that Auger recombination is the low temperature lifetime shortening mechanism.

In what follows, we analyze these ideas in greater detail. In the section **PL Model**, we construct a model of low temperature amorphous semiconductor PL, and in **Results**, we present the predictions of the model. The effect of distant pairs is discussed in **Discussion**.

### PL Model

#### Coulomb assisted recombination

The PL model we suggest is based on the ideas of Coulomb Assisted Recombination. To facilitate the understanding, we summarize here the most important aspects of CAR.

CAR is a low temperature hopping model which takes account of the mutual coulomb interaction between photogenerated electron and hole. The assumptions of the model are as follows. The amorphous semiconductor is modeled as a collection of localized states (sites). The density of localized states is  $N_s$ . The position of each site is random and uniform. The energy ( $E$ ) of each site is also random, and distributed according to an exponential distribution:

$$g(E) = \{1/[\epsilon_0 \exp(E/\epsilon_0)]\} \text{ when } E < 0; \\ = 0 \text{ when } E \geq 0, \quad (9)$$

where  $\epsilon_0$  is the characteristic energy of the distribution. In a-Si:H,  $N_s = 5 \times 10^{19} \text{ cm}^{-3}$  and  $\epsilon_0 = 0.025 \text{ eV}$ .

The density of states,  $N_s$ , defines the characteristic length scale of the lattice of sites,  $a \equiv N_s^{-1/3}$ , which for a-Si:H is 27 Å.

The effect of the electrostatic pair interaction enters as a modification of the site energies. Defining the coordinate origin at the hole, a localized site located a distance  $r$  and with "intrinsic" energy  $E_{\text{intrinsic}}$  in the absence of the hole, has in its presence an effective energy:

$$E = E_{\text{intrinsic}} - \{q/(4\pi\epsilon r)\}, \quad (10)$$

where  $\epsilon$  is the dielectric permittivity and  $q$  is the charge.

After photogeneration of the e-h pair at an initial pair separation  $r_0$ , the carriers begin walking on the lattice of localized sites by tunneling transitions. Since the localization radius of the hole is smaller than that of the electron, the hole is assumed immobile for the duration of the recombination process.

At low temperature, the transition rate between two sites spatially separated by a distance  $R$  is:

$$\nu_{i \rightarrow j} = \{\nu_0 \exp(-2R/\lambda)\} \text{ when } E_i > E_j; \\ = 0 \text{ when } E_i \leq E_j, \quad (11)$$

where  $\nu_0$  is a prefactor on the order of  $10^{12} \text{ s}^{-1}$ , and  $\lambda$  is the localization radius of the localized state. Eq. (11) implies that transitions up in energy are not allowed, in accordance with the low temperature condition. Parallel to the transition to other localized states, a radiative tunneling transition to the hole is also included. For a site at  $r$  from the hole, the transition rate is:

$$\nu_{i \rightarrow \text{hole}} = \{1/\tau_0 \exp(-2r/\lambda)\}. \quad (12)$$

Of great importance is the fact that the transition prefactors obey the inequality

$$(\nu_0 \tau_0) \gg 1, \quad (13)$$

which implies that at equal separation, the electron will jump to a localized site rather than to the hole.

Kemp and Silver (1992) have analyzed the properties of this model. They have shown that as long as the characteristic energy  $\epsilon_0$  of the density of states is small compared with the typical coulomb energy  $\epsilon_{\text{coulomb}} = (q/4\pi\epsilon a)$ , where  $a$  is the characteristic length scale of the lattice of sites ( $a \equiv N_s^{-1/3}$ ), the random walk is strongly biased towards the hole. This is in contrast with the Energy Loss Hopping model of Shklovskii *et al.* (1989), where because of the absence of coulomb interaction, the random walk is diffusive.

The most important consequence of having a biased random walk in the direction of the hole is that the life-

time is solely determined by the separation between the hole and the nearest electronic state to the hole. There are several reasons for this. First, the inequality of eq. (13) implies that all the transitions prior to the actual radiative transition occur very quickly. Therefore, the lifetime depends on the final transition (to the hole) only. Second, because the walk is biased, and because the temperature is low, the electron walks towards the hole, always to a site of lower energy. The walk proceeds until the electron arrives at the localized state with the lowest energy, namely, the site nearest the hole. At this point, the electron is forced to recombine. The crucial point is that the lifetime depends only on the separation between the hole and the nearest electronic state. This separation, because of the randomness of the lattice of sites, is a random variable whose probability density is precisely the nearest-neighbor distribution function:

$$P(r) = \{4\pi N_s r^2 \exp(-4\pi N_s r^3/3)\}. \quad (14)$$

Using the relation between the lifetime and the separation eq. (12), and the properties of the nearest-neighbor distribution function, we arrive at the conclusion that the most probable value of  $\log(\tau)$  is:

$$\log_{10}(\tau)_{\text{peak}} = \{\log_{10}(\tau_0) + (0.47a/\lambda)\}, \quad (15)$$

and that the half-peak width of the distribution is:

$$\Delta_{1/2} \log_{10}(\tau) = (0.44a/\lambda), \quad (16)$$

### Novel model of PL

The data show there are two lifetime peaks, at  $3 \times 10^{-6}$  s and  $3 \times 10^{-3}$  s. The widths of the peaks are about 2 decades. At low generation rate, the ratio of fast over slow recombination is 1:3. The data also shows that the efficiency is not unity at large generation rate.

The most important shortcomings of CAR are that (i) it predicts one lifetime peak only. Assuming the typical values  $\tau_0 = 6 \times 10^{-7}$  s and  $\lambda = 18 \text{ \AA}$ , the lifetime peak occurs at  $3 \times 10^{-6}$  s; (ii) it assumes unit efficiency, independent of the generation rate. The advantage of CAR is that it predicts the correct peak width. As we mentioned it in the Introduction, the fact that the CAR width is comparable with the experimental width gives strong argument in favor of including explicitly the coulombic pair interaction. However, since CAR is not exempt from other problems, it needs be extended.

The first important piece of information is that the two lifetimes differ by three orders of magnitude, and that they occur in a ratio of 1:3. This is reminiscent of spin selection effects. Including spin selection effects means, we recognize the allowed transition as singlet recombination and the forbidden as a triplet. Assuming

the recombination time is longer than the spin flip time, triplet recombination is 3 times more probable than singlet:

$$\begin{aligned} P_{\text{triplet}} &= 3/4 \\ P_{\text{singlet}} &= 1/4. \end{aligned} \quad (17)$$

Without going into quantum mechanical calculations, it is not possible to estimate the radiative recombination rates. We can safely assume that the dependence on pair separation will be the same as that in eq. (12), and that because of spin selection, the prefactor  $\tau_0$  can assume two values instead of only one:

$$\begin{aligned} \nu_{i \rightarrow \text{hole}} &= \\ &\{1/\tau_0^s \exp(-2r/\lambda)\} \text{ singlet recombination; and} \\ &\{1/\tau_0^t \exp(-2r/\lambda)\} \text{ triplet recombination.} \end{aligned} \quad (18)$$

In Determination of the model parameters, we will see how experiment enables a unique determination of  $\tau_0^s$ , and  $\tau_0^t$  and  $\lambda$ .

The second important piece of data is the reduction in efficiency at high generation rate. This, of necessity, implies that a non-radiative pathway must be included on top of the radiative channel already present in CAR. The  $G^{-1/2}$  high G dependence of the efficiency implies that the rate of non-radiative recombination is proportional to the carrier density

$$\nu_{\text{non-radiative}} = An, \quad (19)$$

where A is a proportionality constant, and n the carrier density. This type of dependence is reminiscent of Auger recombination. Auger recombination is a process whereby an electron-hole pair recombines by giving its energy to other electrons and holes. The transfer of energy is easier when the density of carriers is large, which explains the dependence on carrier density.

Similar to radiative recombination, the rate of energy transfer depends on the spin state of the recombining pair. This enters as a spin dependence of the rate prefactor A, which can now assume two values:

$$\begin{aligned} \nu_{\text{non-radiative}} &= \\ &A^t n \text{ triplet recombination; and} \\ &A^s n \text{ singlet recombination.} \end{aligned} \quad (20)$$

As before, the values of  $A^s$  and  $A^t$  cannot be derived without calculations, but we will show in Determination of the model parameters how to determine them uniquely from experiment.

### Lifetime distribution and PL intensity

The ideas expressed in the previous two sections permit the calculation of the lifetime distribution and of the PL intensity. After photogeneration, the electron walks down in energy until it occupies the nearest electronic site to the hole. The pair separation at this point is  $r$ , where  $r$  is a random variable with distribution

$$P(r) = \{4\pi N_s r^2 \exp(-4\pi N_s r^3/3)\}. \quad (21)$$

Given a specific realization  $r$  of the pair separation, the electron can either recombine radiatively or non-radiatively. Radiative recombination occurs in the triplet state with probability  $3/4$ , and the singlet state with probability  $1/4$ . The non-radiative process competes with the radiative one, and forces long-lived pairs to recombine non-radiatively. Given a generation rate  $G$ , the steady-state carrier density is:

$$n = G \cdot \int_0^\infty \{drP(r)\} \cdot \left\{ \frac{3}{4} \left[ \frac{1}{1/\tau_0^t \exp(-2r/\lambda) + A^t n} \right] + \frac{1}{4} \left[ \frac{1}{1/\tau_0^s \exp(-2r/\lambda) + A^s n} \right] \right\}. \quad (22)$$

The PL intensity is:

$$PL = G \cdot \int_0^\infty \{drP(r)\} \cdot \left\{ \frac{3}{4} \left[ \frac{1/\tau_0^t \exp(-2r/\lambda)}{1/\tau_0^t \exp(-2r/\lambda) + A^t n} \right] + \frac{1}{4} \left[ \frac{1/\tau_0^s \exp(-2r/\lambda)}{1/\tau_0^s \exp(-2r/\lambda) + A^s n} \right] \right\}. \quad (23)$$

Note that the first equation is self-consistent, since both the factor that multiplies the generation rate and the left-hand-side depend on  $n$ . After solving eq. (22) for a given generation rate, the steady-state charge density is used in eq. (23) to find the PL intensity.

The ratio of the PL intensity over the generation rate is the total efficiency. The efficiency consists of two additive contributions, the triplet and the singlet, which permits an unambiguous assignment of a triplet and a singlet efficiency.

The efficiency also permits the determination of the distribution of  $x \equiv \log_{10}(\tau)$ . The singlet contribution to the distribution is obtained by making the change of variables:

$$10^{-x} = \{A^s n + 1/\tau_0^s \exp(-2\tau^s(x)/\lambda)\}, \quad (24)$$

and substituting  $r^s(x)$  in the singlet integrand of eq. (23). Similarly, the triplet contribution is found by using:

$$10^{-x} = \{A^t n + 1/\tau_0^t \exp(-2\tau^t(x)/\lambda)\}. \quad (25)$$

Using these variables in the PL expression eq. (23), the distribution of  $x$  becomes:

$$\phi(x) = \left\{ \frac{3}{4} [P(r^t(x))] + \frac{1}{4} [P(r^s(x))] \right\}. \quad (26)$$

We point out that the distribution  $\phi(x)$  is not normalized to unity, but to the efficiency  $PL/G$ . This definition is the experimental standard, since  $\phi(x)$  is the quantity that is directly measured by QFRS.

The lifetime peaks are easily derived from eq. (26). Using the properties of the nearest-neighbor function  $P$ , the peaks occur at:

$$x_{\text{peak}} = \begin{cases} \{-\log_{10}(A^t n + 1/\tau_0^t \exp(-0.54 \cdot 2a/\lambda))\} & \text{triplet;} \\ \{-\log_{10}(A^s n + 1/\tau_0^s \exp(-0.54 \cdot 2a/\lambda))\} & \text{singlet.} \end{cases} \quad (27)$$

### Results

#### Determination of the model parameters

The precise values of  $\tau_0^s$ ,  $\tau_0^t$  and  $\lambda$  can be determined directly from the experimental values. First, using eq. (16), along with the fact that the QFRS method gives a total width equal to the lifetime width plus a QFRS broadening of 1.5 decade, and the observed width is 2 decades, we derive  $a/\lambda = 1.5$ . Second, using the experimental lifetime peak values in eq. (18)

singlet recombination:

$$\tau^s = 3 \cdot 10^{-6} \text{ s} = \tau_0^s \exp(2 \cdot 0.54 a/\lambda)$$

triplet recombination:

$$\tau^t = 3 \cdot 10^{-3} \text{ s} = \tau_0^t \exp(2 \cdot 0.54 a/\lambda), \quad (28)$$

and substituting the value of  $(a/\lambda)$  in eq. (28), we get  $\tau_0^s = 6 \times 10^{-7} \text{ s}$  and  $\tau_0^t = 6 \times 10^{-4} \text{ s}$ .

These values are larger than the values which are usually assumed ( $\lambda = 10 \text{ \AA}$  and  $\tau_0 = 10^{-8} \text{ s}$ ). We point out in defense of the values we suggest that those which are usually assumed were arrived at by a procedure identical to ours, with the difference that the pair separation was assumed to be  $50 \text{ \AA}$ . This value of  $50 \text{ \AA}$ , we emphasize, is still without any form of theoretical support.

The values of  $A^s$  and  $A^t$  can also be derived by comparison with experiment. The transition from radiative to Auger dominated recombination occurs at {eq. (8)}:

$$G^{(\text{triplet})} = 1/A^t (\tau^t)^2. \quad (29)$$

Using the fact that the electron density is mostly in the triplet state (since the triplet lifetime is much longer than the singlet), the equivalent equation for the singlet transition to Auger dominated recombination is:

$$G^{(\text{singlet})} = A^t / (A^s \tau^s)^2. \quad (30)$$

## Monte-Carlo CAR

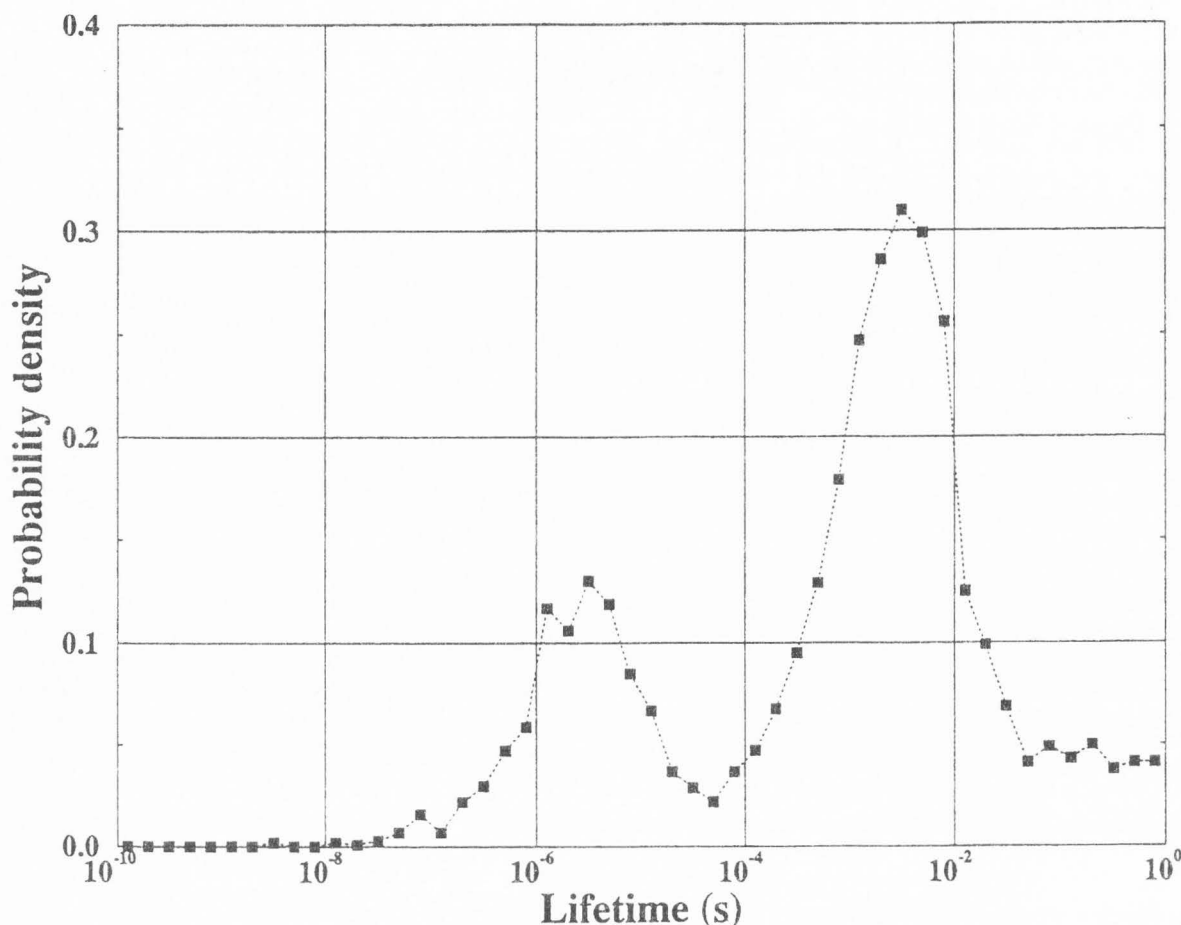


**Figure 1.** Probability density of the logarithm of the lifetime predicted by the model of Coulomb Assisted Recombination (CAR). The curve was obtained by running Monte-Carlo simulations following the procedure described in Kemp and Silver (1992) with the difference that recombination occurs in the triplet state with a probability of 3/4, and in the singlet, with a probability of 1/4. The simulation assumes unit radiative efficiency. The simulation parameters are those of Determination of the model parameters.

Experiments show that the triplet Auger transition occurs at  $G^{(\text{triplet})} = 10^{19} \text{ cm}^{-3} \text{ s}^{-1}$  and the singlet at  $G^{(\text{singlet})} = 10^{22} \text{ cm}^{-3} \text{ s}^{-1}$ . Using eqs. (29) and (30), this gives  $A^s = 10^{-14} \text{ cm}^3 \text{ s}^{-1}$  and  $A^t = 3 \times 10^{-13} \text{ cm}^3 \text{ s}^{-1}$ .

### Lifetime distribution

Figure 1 shows the lifetime distribution predicted by CAR. This figure is arrived at by running a Monte-Carlo simulation using the procedure described in Kemp and Silver (1992). This simulation assumes the absence of any non-radiative process, but consistent with the ideas expressed in PL Model, triplet recombination occurs with a probability of 3/4 and singlet with a probability of 1/4. The model parameters are those of Determination of the model parameter.

The figure shows there are two lifetime peaks, at  $3 \times 10^{-6} \text{ s}$  and  $3 \times 10^{-3} \text{ s}$ , and that the ratio of triplet to singlet peak height is about 3:1. The half-peak width of both peaks is about 2 decades (note: the simulation procedure gives a broadening equivalent to QFRS). The internal simulation variables reveal that the recombination lifetime is determined by the radiative transition in over 99% of the cases. This implies that the lifetime distributions is described by the nearest-neighbor distribution function, in agreement with the ideas expressed in PL Model.

The low  $G$  lifetime distribution calculated using eq. (26) (that is, incorporating the effect of Auger recombination) is shown in Figure 2. The "pure" distribution is that arrived at using eq. (26) directly. The "convoluted"

## Lifetime distribution

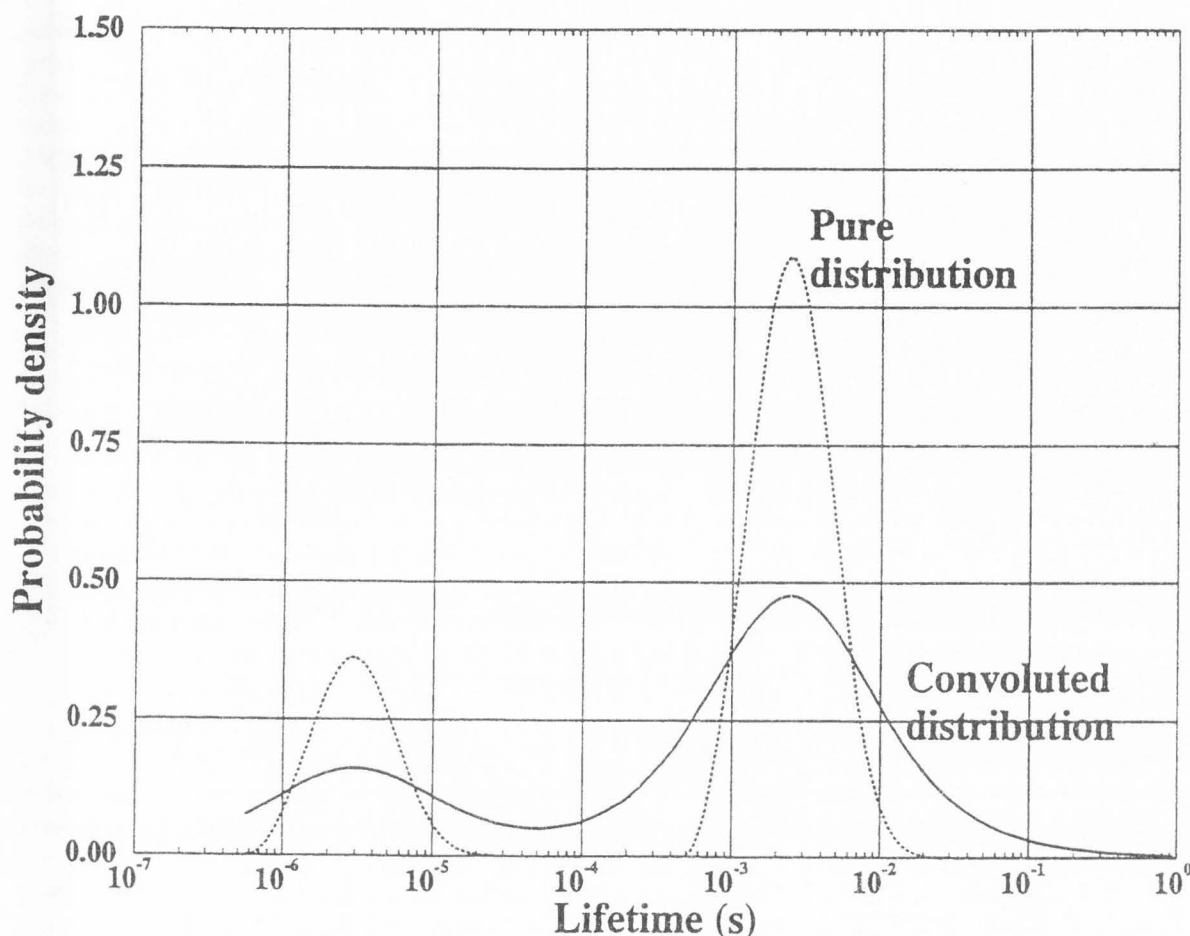


Figure 2. Low generation rate probability density of the logarithm of the lifetime, computed using eqs. (22-26) with the parameters of Determination of the model parameters. The dashed line corresponds to the pure lifetime distribution, eq. (26); the solid line is obtained by convolution of the dashed line with the QFRS scan function eq. (31).

distribution is arrived at by convoluting the "pure" distribution with the QFRS scan function (Stachowitz *et al.*, 1993):

$$\{[\phi_{\text{convoluted}}][x = \log_{10}(\tau)]\} = \{[2/\pi \log(10)] \cdot \int_0^{\infty} [(\phi(y)dy)/(10^{x-y} + 10^{y-x})]\}. \quad (31)$$

The convoluted distribution is the one that should be compared with experiment. Both the pure and the convoluted distribution show two peaks, at  $3 \times 10^{-6}$  s and  $3 \times 10^{-3}$  s. The ratio of the triplet to the singlet peak height is 3:1. The half-peak width of the pure distribution is about 0.7 decades, whereas the width of the convoluted is 2 decades. This extra broadening is the direct result of the QFRS scan function (an extra 1.5 decades).

Probably the most significant feature of Figure 2 is the fact that the pure lifetime broadening is very small.

In accordance with our interpretation of the data, the lifetime broadening is inversely proportional to the localization radius of the electronic states. Whereas the observed width would lead to the conclusion that the localization radius is about 6 Å, the fact that a large fraction of the width is due to the experimental procedure implies a much larger localization radius. Figure 2, and its agreement with experiment, implies that the localization radius is in fact of order 18 Å.

#### Dependence on generation rate

The dependence of the lifetime peaks on the generation rate  $G$  is shown in Figure 3. For either the triplet or the singlet channel, the lifetime is constant at low generation rate, and decreases as  $G^{-1/2}$  goes above a threshold value. The singlet threshold occurs at  $10^{22}$   $\text{cm}^{-3}\text{s}^{-1}$ , and the triplet at  $10^{19}$   $\text{cm}^{-3}\text{s}^{-1}$ .

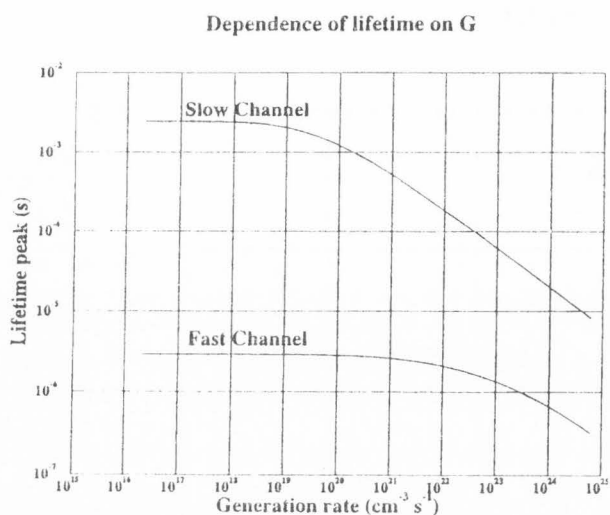


**Figure 3.** Dependence of the lifetime peaks on generation rate. The slow channel is associated with triplet recombination, the fast channel with singlet.

The dependence of the triplet and singlet PL intensities on generation rate, as well as that of the lifetime peaks, are shown in Figure 4 (the lifetimes have been shifted to coincide with the low  $G$  efficiencies). The first dominant feature in this figure is the fact that the efficiencies and the lifetime peaks behave identically. The second important fact is that singlet recombination is the dominant recombination mechanism for generation rates in excess of  $10^{21} \text{ cm}^{-3} \text{ s}^{-1}$ , whereas triplet recombination dominates at small generation rate.

### Discussion

#### Implications of the model

The agreement of the model predictions with experiment warrants some interesting implications:

(i) The existence of two peaks is a consequence of spin selection rules. This is a highly testable assumption. It would be interesting to repeat the low temperature experiment (2 K) in the presence of a magnetic field. According to our model, the field should quench the triplet contribution; so at high fields, only singlet recombination should be observed (fast lifetime only).

(ii) The localization length of the electronic states is directly measurable from the width of the lifetime distribution. However, we point out that only the "pure" distribution contains information on the localization length; the QFRS spectra should therefore be deconvoluted first. Also, the width of the distribution decreases with increased generation rate, this because the Auger mechanism affects mostly the slowest pairs. The width of the fast peak, because it is less susceptible to Auger,

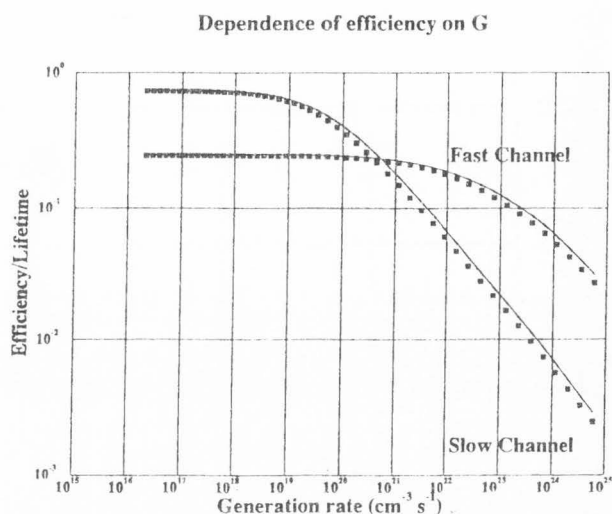


**Figure 4.** Dependence of the efficiency on generation rate. The solid lines are the efficiencies of the triplet (slow) and of the singlet (fast) channels. The dependence of the lifetime peaks on  $G$  (diamonds) is also shown. For comparison, the lifetimes have been shifted to coincide with the low generation rate efficiencies.

should therefore be more appropriate to a measurement of the localization radius.

(iii) The radiative prefactors can also be measured from the peak positions, granted the localization radius has been measured.

(iv) The shape and peak positions of the lifetime distribution is insensitive to the details of the density of states. This arises because the distribution depends on the nearest-neighbor distance only, which is a universal function of the total density of states only. We therefore submit that similar behavior should be observable in all amorphous semiconductors where spin selection effects are important.

(v) The shortening of the lifetime with increased generation rate is not due to non-geminate recombination, as has been assumed until now. Rather, it is the result of non-radiative recombination. It is not absolutely clear whether this mechanism is Auger recombination or not. The only unambiguous feature of this process is that its rate increases linearly with photocarrier density, which is a feature of Auger. Other mechanisms are, however, possible.

#### Effect of distant pairs

The distant-pair model can explain some of the experimental features, however, not most of them. On the other hand, one might question the validity of our model in neglecting distant-pairs altogether. The Monte-Carlo simulation that was used to derive Figure 1 shows that

the fraction of pairs that escape the coulombic attraction is of order 10%, independent of the initial pair separation. This signifies that even though the coulomb interaction drives the recombination dynamics of most photo-generated pairs, there are pairs which do escape the coulombic influence. The electrons of these pairs move down in energy, until they occupy low energy sites. Having dissociated from their sibling hole, they give rise to a 20 metastable population of randomized and immobile carriers. Those are precisely the assumptions of the distant pair model, which suggests that we examine this effect in greater detail.

Levin *et al.* (1992) have examined the distant pair model by Monte Carlo methods. They have shown that a distant pair generation rate  $G_{DP}$  gives rise to a the steady-state density of distant-pair carriers:

$$n_{DP} = G_{DP} \tau_o \exp(0.51 \cdot 2n_{DP}^{-1/3}/\lambda). \quad (32)$$

Note the presence of the prefactor  $\tau_o$ , which stems from their assumption that DP recombination is the result of a direct radiative transition. We believe this to be inappropriate because of the coulomb interaction. The coulomb interaction modifies the site energies and is especially important for sites in the vicinity of a carrier. The energy pull-down might be as large as 0.05-0.2 eV for near states. Consider now a distant electron that is to recombine with a hole. The electron can either (i) recombine in one radiative step, and pay the price of the condition  $\nu_o \tau_o \gg 1$ , or (ii) it can go in two steps, first to a localized site in the vicinity of the hole, and second radiatively, this time from short range. Process (ii) is much faster than (i)  $\nu_o \tau_o \gg 1$ . We therefore suggest that because of the coulomb interaction, distant pair recombination is a two-step process.

The effect of DP can be incorporated in the model we have discussed by splitting the total carrier population ( $n$ ) in two, the close-pair (CP) population ( $n_{CP}$ ) and the distant-pair population ( $n_{DP}$ ):

$$n = n_{CP} + n_{DP}. \quad (33)$$

Assuming that 90% of the pairs are created as close-pairs, the steady-state populations obey:

$$n_{CP} = 0.9G \cdot \int_0^\infty \{drP(r)\} \cdot \left\{ \left[ \frac{3}{4} \right] \left[ \frac{1}{1/\tau_o^t \exp(-2r/\lambda)} + A^t n \right] + \left[ \frac{1}{4} \right] \left[ \frac{1}{1/\tau_o^s \exp(-2r/\lambda)} + A^s n \right] \right\} \quad (34)$$

and

$$n_{DP} = 0.1G \cdot \left\{ \tau_{DP}(n_{DP}) + \int_0^\infty \{drP(r)\} \cdot \left\{ \left[ \frac{3}{4} \right] \left[ \frac{1}{1/\tau_o^t \exp(-2r/\lambda)} + A^t n \right] + \left[ \frac{1}{4} \right] \left[ \frac{1}{1/\tau_o^s \exp(-2r/\lambda)} + A^s n \right] \right\} \right\}, \quad (35)$$

Total vs distant pair charge

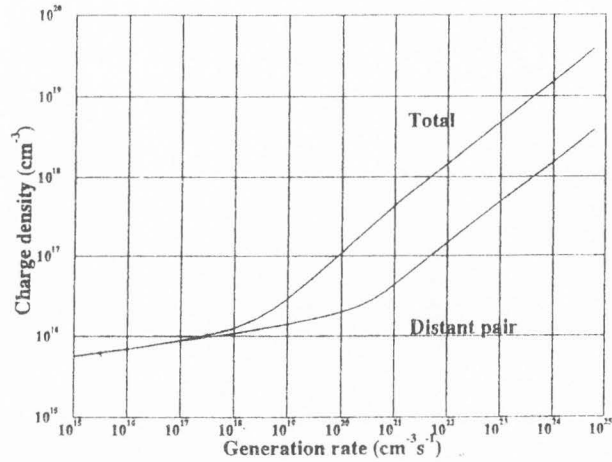


Figure 5. Dependence of the charge density on generation rate, when the effect of distant pairs is included. At low  $G$ , distant pairs contribute the quasi-totality of the charge density; at large  $G$ , distant pairs are negligible compared with the total charge. The transition between the two regimes occurs around  $G = 10^{17} \text{ cm}^{-3} \text{ s}^{-1}$ .

where

$$\tau_{DP}(n_{DP}) = \left\{ 1/\nu_o \exp(0.51 \cdot 2n_{DP}^{-1/3}/\lambda) \right\}. \quad (36)$$

Eq. (34) contains the fact that Auger recombination depends on the total carrier density. Eq. (35) expresses the fact that the first DP step is a jump to the nearest-neighbor to the hole, and that the radiative event occurs exactly as it does for close-pairs. These equations are coupled in the Auger term, so that they must be solved simultaneously.

The dependence of the total and distant-pair carriers densities on generation rate is shown in Figure 5. This shows that at low generation rate, distant-pairs control the total population, but that for larger  $G$ , the distant-pair effect is negligible. This result can be understood as follows. At low generation rate, the carrier population is small. Since the DP rate is very small in this case {eq. (36)}, the DP population builds up until it catches up with the DP generation rate. Close-pairs on the other hand, have a much shorter lifetime, and quickly saturate to their steady-state value. As the generation rate is increased, the DP pair population increases, but very slowly, whereas the CP population increases linearly with  $G$ . The CP and DP populations are equal at a generation rate  $G_{DP}$ . For generation rates above  $G_{DP}$ , distant pairs can be neglected.

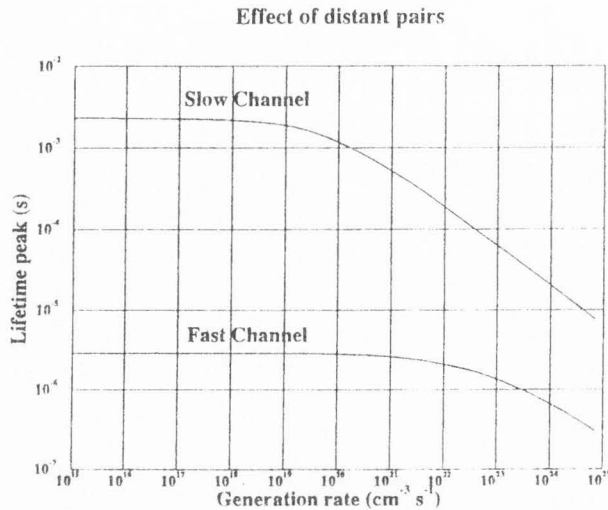


**Figure 6.** Effect of the distant pairs on the G lifetime peak dependence. The effect is minimal, as can be seen by direct comparison with Figure 2.

The only question that remains is whether distant pairs affect the recombination lifetime at all. The radiative lifetime can only change because of a non-radiative process. Therefore, we must compare  $G_{DP}$  with  $G^{triplet}$ . Figure 5 shows that  $G_{DP}$  lies around  $10^{17} \text{ cm}^{-3} \text{ s}^{-1}$ , about 100 times smaller than  $G^{triplet}$ . Therefore, the distant pair population has only a minimal effect on the lifetime distribution. This is further documented in Figure 6.

Measurable consequences of having a combination of close and of distant pairs should be apparent in the transient behavior of the PL signal:

(i) When the optical excitation is switched on: At low G, the PL intensity should increase rapidly, on the time scale of the triplet lifetime ( $10^{-3}$  s). The total carrier density on the other hand should rise with the DP lifetime. For a generation rate  $G = 10^{16} \text{ cm}^{-3} \text{ s}^{-1}$ , the carrier rise time should be on the order of 10-100 seconds. At high G, the DP population is larger and the rise time much shorter (about  $10^{-3}$  s). These predictions are all consistent with experiment (Bort *et al.*, 1991).

(ii) When the light is switched off. At low G, the decay of the PL signal should be fast ( $10^{-3}$  s), but the decay of the carrier density is slow, since it is controlled by the DP population. At high G, the PL signal should decrease quickly and be accompanied by a large reduction of the carrier population. After this fast initial decay of close pairs, a slow decay of the distant pair population should follow. This is also borne out by experiment (Bort *et al.*, 1991).

Ambros S, Carius R, Wagner H (1991) Lifetime distribution in a-Si:H: Geminate, nongeminate and Auger processes. *J Non-Cryst Solids* **137-138**: 555-558.

Bort M, Fuhs W, Liedtke S, Stachowitz R (1991) Geminate recombination in a-Si:H. *Phil Mag Lett* **64**: 227-233.

Dunstan DJ (1982) Kinetics of distant-pair recombination I-Amorphous silicon luminescence at low temperature. *Phil Mag* **B46**: 579-594.

Kemp M, Silver M (1992) A Monte-Carlo investigation of low-temperature geminate pair recombination dynamics in amorphous semiconductors. *Phil Mag Lett* **66**: 169-174.

Levin EI, Marianer S, Shklovskii BI (1992) Photoluminescence of amorphous silicon at low temperatures: Computer simulation. *Phys Rev* **B45**: 5906-5918.

Shklovskii BI, Fritzsche H, Baranovskii SD (1989) Electronic transport and recombination in amorphous semiconductors at low temperatures. *Phys Rev Lett* **69**: 2989-2992.

Stachowitz R, Schubert M, Fuhs W (1993) Frequency-resolved spectroscopy and its application to lifetime studies in a-Si:H. *J Non-Cryst Solids* **164-166**: 583-586.

Street RA (1984) Luminescence in a-Si:H. In: *Hydrogenated Amorphous Silicon: Semiconductor and Semimetals*. Vol. 21B. Pankove JI (ed.). Academic Press, New York. pp. 197-244.